Artificial Intelligence Technique for the Work Hardening Characteristics of Al-Si Alloy

A. M. Abd El-Khalek*[a,b], R.H. Nada[b], M. Y. El-Bakry[a,b], Taymour A. Hamdalla[a,c], Said A. Farha Al-Said[a,d], and A. E. Bekheet[a,b]

a. Physics Department, Faculty of Science, University of Tabuk, Tabuk, Saudi Arabia
b. Physics Department, Faculty of Education, Ain Shams University, Cairo, Egypt
c. Physics Department, Faculty of Science, Alexandria University, Alexandria, Egypt
d. Physics Department, King Abdulaziz University, Jeddah, Saudi Arabia.

a.elkhalek@ut.edu.sa Tel.: 00966593554325

Abstract— Stress -strain curves were carried out in the temperature range from 493K to 553K for Al-1wt%Si alloy samples containing the α-solid solution phase and irradiated with γ -doses up to 1.75 MGy. The measured parameters: fracture strain rate ε_f, fracture stress σ_f, yield stress σ_y, coefficient of work hardening, χ and the obtained TEM micrographs showed increasing hardness up to 523K after which softening took place. Irradiation was indicating a compensated effect at any testing temperature. To model the work hardening characteristics of Al-Si alloy, the artificial neural networks (ANNs) technique was used. The results of ANN demonstrate the feasibility of such technique in extracting the hardening parameters and prove its effectiveness.

Index Terms— Stress-Strain, Gamma-rays, Irradiation, Dislocation, Work hardening, Softening, Artificial neural network..

1 INTRODUCTION

Mechanical properties of aluminum can be improved by alloyin g, strain hardening, thermal treatment or by combination of the three techniques[1-4].

The Al–Si alloys are widely used in the automotive and aerospace industries, where they have been steadily replacing many conventional ferrous alloys due to their excellent combination of properties such as good fluidity, low coefficient of thermal expansion, high strength-to-weight ratio, good corrosion resistance and minimum energy requirement for recycling.

In a quenched Al–Si alloy, silicon precipitates nucleate on vacancy clusters and dislocation loops [5]. Si precipitates become visible after the disappearance of the formed dislocation loops. The nucleation of Si precipitates was enhanced by pre-ageing quenched specimens near room temperature as a result of the existence of the dislocation loops formed by the condensation of the quenched alloy in vacancies [6]. Studies of structure and mechanical properties of low silicon–aluminium alloys were carried out [7, 8]. Both strength and ductility of the alloy were functions of the size and distribution of the Si particles in the aluminium matrix [9].

In the Al–Si alloys, the solubility of Si in aluminum is negligible below 523 K [10], therefore separate phase exists. Above 523 K, the process of Si precipitation cease and, consequently, a reduction in the microhardness of these alloys is observed above 573 K [11].

Ionizing radiation is known to be one of the major sources for altering the internal structure of crystalline metallic materials and consequently their properties, that are largely governed by lattice defects [12]. Therefore, attention is focused on irradiation effects to search for new materials that can withstand radiation damage[12]. On the other hand, we try to use the artificial neural network (ANN) [13-17] technique to model the hardening characteristics of Al-Si alloy. The ANN model is chosen for his ability to perform complex functions in various fields of application including pattern recognition, modeling, identification, classification, speech, vision and control systems [18].

It is well known [19-22], in fact, that multilayer neural network with sigmoidal activation neurons an n-input neurons can approximate any nonlinear, n-dimensional function, with a precision that depends only on the number of hidden neurons.

The aim of the present work is to investigate the effect of temperature and gamma-rays irradiation on the work hardening characteristics of Al-1wt%Si alloy as in section 4.1. Section 4.2, introduce the development in the artificial neural network (ANN) and describe the manner of modeling and simulation the parameters: fracture strain rate ε_f, fracture stress σ_f, yield stress σ_y, and coefficient of work hardening, χ.

2 EXPERIMENTAL PROCEDURE:

Al-1wt%Si alloy was prepared by melting 99.99% pure aluminum and 99.98% Si in a clean graphite crucible in a vacuum induction furnace. The cast ingot was homogenized under vacuum of 10^{-3} Torr, at 823 K for 48 h and then cold drawn to

wires of 2 mm diameter. The wires were given intermediate annealing treatment at 773 K for 6 h then cold drawn in diamond dies down to wires of 0.4 mm in diameter and 5 cm length. All the specimens were solution treated for 2 h at 823 K, then quenched into water kept at room temperature (RT~ 300K) to get samples containing the α-solid solution phase. The samples were irradiated with different doses of gamma radiation up to 1.75 MGy. In the ^{60}Co gamma rays cell used, the dose rate was 1.58 KGy/min.

Stress - strain tests were carried out with an average strain rate of 2×10^{-2} S^{-1} in the temperature range from 493 K to 553 K. The load applied to the sample was gradually increased by adding 200 g, with 30 second between each two successive loadings and the elongation was immediately recorded before the next loading. The elongations were measured by a dial gauge to an accuracy of $\pm 10^{-5}$ m. The yield stress, σ_y is considered to be the stress corresponding to the first significant deviation from linearity in the starting part of the stress - strain curve. The maximum stress applied to the sample before fracture was taken as the fracture stress σ_f [23]. The microstructure of the Al-1wt% Si alloy was investigated using a joel 100S electron microscope working at 100 kV.

3. Modeling The hardening characteristics of Al-Si alloy using ANN:

The ANN technique is described in detail in [13-17, 18-20]. The main ideas are summarized here.

3.1. Basic principle:

An artificial neural network (ANN) consists of a number of very simple and highly interconnected computational elements, also called neurons or nodes (Fig. 1).

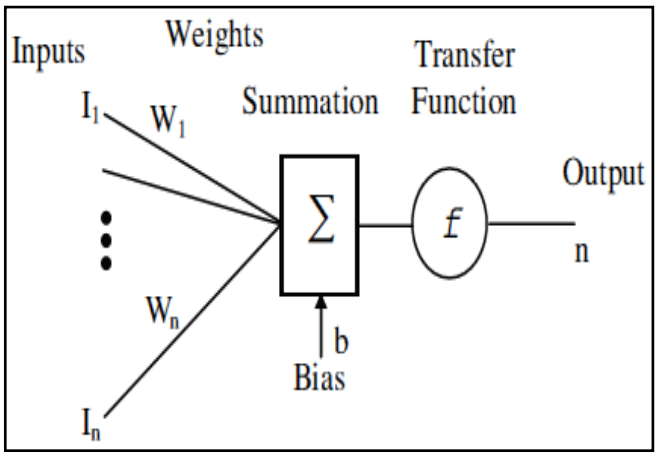

Fig. 1, Neuron structure

These nodes are distributed on many different layers: (a) one input layer, (b) one or many hidden layers and (c) one output layer.

The processing element calculates the neuron transfer function (f) of the summation of weighted inputs. The neuron transfer function, f, is typically step or sigmoid function that produces a scalar output as in eq. (1):

$$n = f(\Sigma_i W_i I_i + b) \quad (1)$$

where I_i, W_i, b are the i th input, the i th weight and b the bias respectively.

A particular transfer function (f) is chosen to satisfy some specification of the problem that the neuron is attempting to solve. The most commonly used functions is the tansigmoid and logsigmoid transfer function.

3.2. Training of the ANN Model:

For training the neural network, a vector in the data matrix is a pattern. Each pattern is given to the network and the output is compared with the response. The data set is randomly divided into training and test sets. The error function is calculated after all the patterns are presented. Hence, it is a supervised learning. The best architecture (Fig. 2) is chosen by changing the number of hidden layers, hidden neurons in each layer, transfer function and learning algorithm.

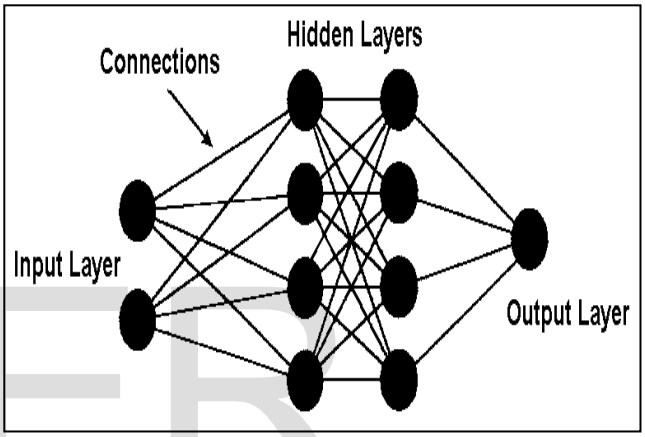

Fig. 2- Multilayer perception neural network architecture

The widely employed optimization procedure (learning algorithm) in 1980, was back propagation (BP), which is a variation of steepest descent algorithm. Recently Marquardt, Conjugate Gradient, simulation annealing algorithm, Genetic algorithm, etc. have been in corporated in ANN software.

4. Results and Discussion:

4.1. Experimental Results:

The stress-strain relations for Al-1wt%Si alloy samples irradiated with different γ-doses (0, 0.6, 1, 1.2 and 1.75 MGy) obtained at different working temperatures. From the stress - strain curves the following parameters were measured: fracture strain rate ε_f, fracture stress σ_f, yield stress σ_y, and coefficient of work hardening, χ. The temperature dependence of these parameters for samples irradiated with different doses is given in Fig. 3, and electron micrographs showing Si precipitates in Al-1wt%Si alloy heated for 3 h at 423, 523 and 623 K are given in Fig. 4(a - c). It is clear from Fig. 3 that there exists a critical temperature (523 K) characterizing two opposite behaviours for the observed variations in the measured parameters.

The nucleation of precipitates in Al-Si alloys was enhanced by pre-aging quenched specimens near room temperature [24]. Such enhancement can be attributed to dislocation loops formed by condensation of quenched - in vacancies. Observations showed [9] that Si precipitates nucleated on vacancy clusters, but their formation and the subsequent nucleation took place within a few seconds after quenching.

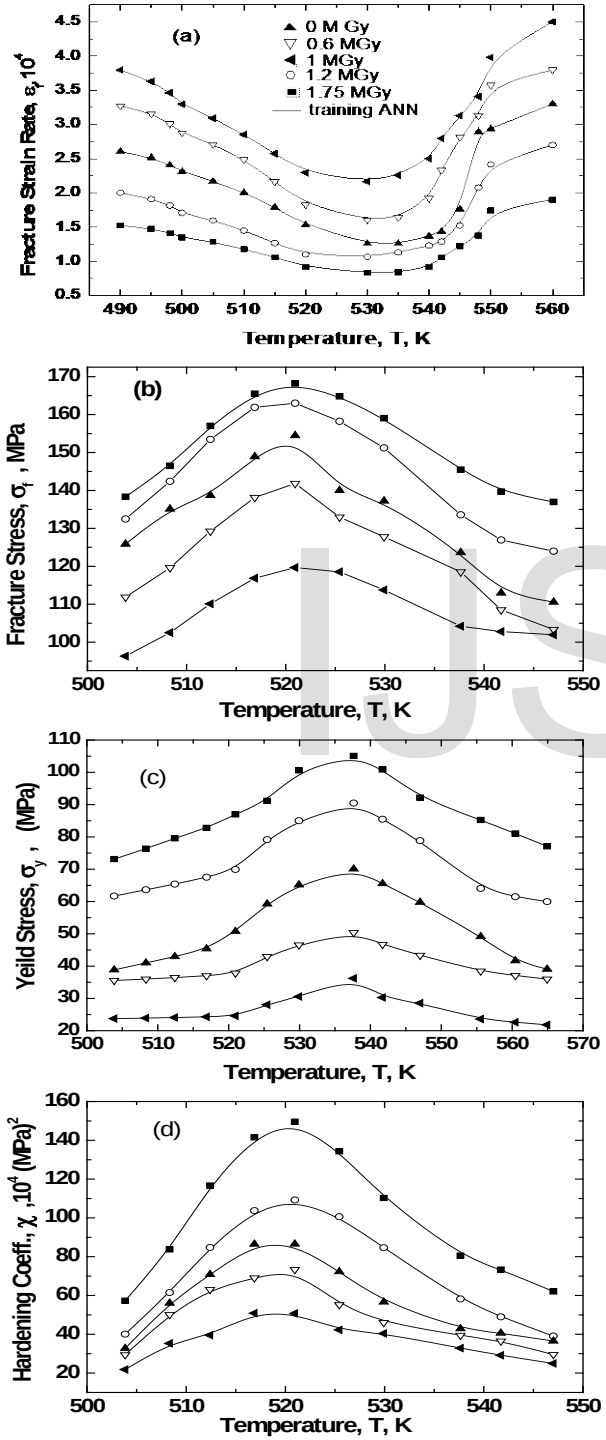

Fig. 3- The temperature dependence of :a) fracture strain rate, ε_f, b) fracture stress, σ_f c) yield stress, σ_y and d) Hardening coefficient, χ, for irradiated samples with the indicated doses.

At relatively lower temperatures, below 523 K, heterogeneous precipitation may take place by the motion of vacancy-Si atom pairs. The Si concentration might reach its equilibrium value due to the saturation of the heterogeneous nucleation sites. Although this process makes the matrix of the alloy poor in Si atoms, yet Si concentration remains still higher than the equilibrium value. The remaining supersaturation of the matrix can thus be removed by homogeneous nucleation leading to zone formation responsible for the observed hardening for samples annealed at temperatures below 523 K. This hardening shows itself in Fig.3 as an increase in all the hardening parameters such as: σ_y, σ_f and χ reaching maxima at 523 K and a decrease in ε_f to minima at 523 K. This is supported by the TEM micrographs of Fig. 4 (a, c) where the maximum hardness corresponds to the high precipitate density observed in Fig. 4b.

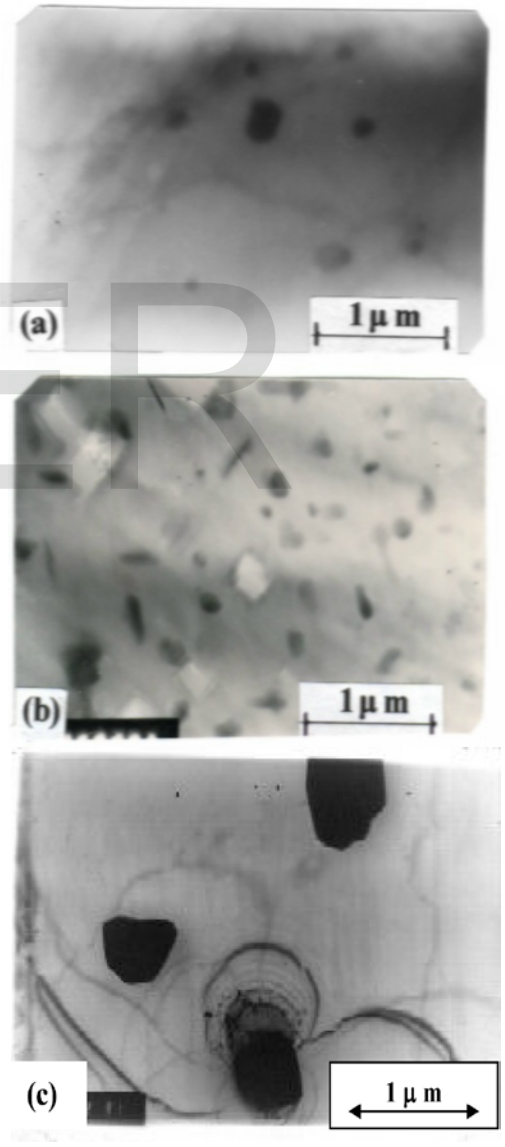

Fig. 4 : Electron micrographs showing Si precipitates in Al - 1wt%Si alloy heated for 3 h at (a) 423 K (b) 523 K and (c) 623 K.

As the working temperature exceeds 523 K, the zones may be rather unstable and they can easily transform to nuclei of precipitates if the Si concentration of the matrix is not too low and the temperature is relatively high. The Si atoms in the zones can collapse to form precipitates, with sizes increasing with the working temperature (see Fig. 4c), leading therefore to a decrease in hardness. This decrease in hardness, or softening of the alloy, is reflected through the observed decrease in the hardening parameters σ_f, σ_y and χ and an increase in ε_f given in Fig. 3. The thermally induced internal structure of the alloy in the tested temperature range which leads to the observed hardening behaviour up to 523 K after which a softening behaviour dominates, consists with previous studies [25].
Irradiation damage caused by γ -rays creates ionizing type defects of densities depending on the radiation dose. The observed softening might be the result of the induced irradiation defects interaction with the existing quenching defects which leads to the annihilation of many defects at different sinks in the matrix. Also, the precipitating Si atoms on dislocations might be liberated and the pinned dislocations contribute to the density of mobile dislocations, which leads to the observed softening.

4.2. Simulation Results:

The proposed ANN model of hardening characteristics of Al-1wt%Si alloy, is simply shown as two-inputs one-output model, Fig.5. The inputs are: the different working temperatures (490 – 560 K) and the different γ- doses (0, 0.6, 1, 1.2 and 1.75 MGy), while the output is: fracture strain rate ε_f, fracture stress σ_f, yield stress σ_y, or coefficient of work hardening, χ.
As the nature of the output (ε_f, σ_f, σ_y, or χ) is completely different from each other, authors choose to internally model the problem with four individual NN trained separately using experi
mental data as described in the above section.

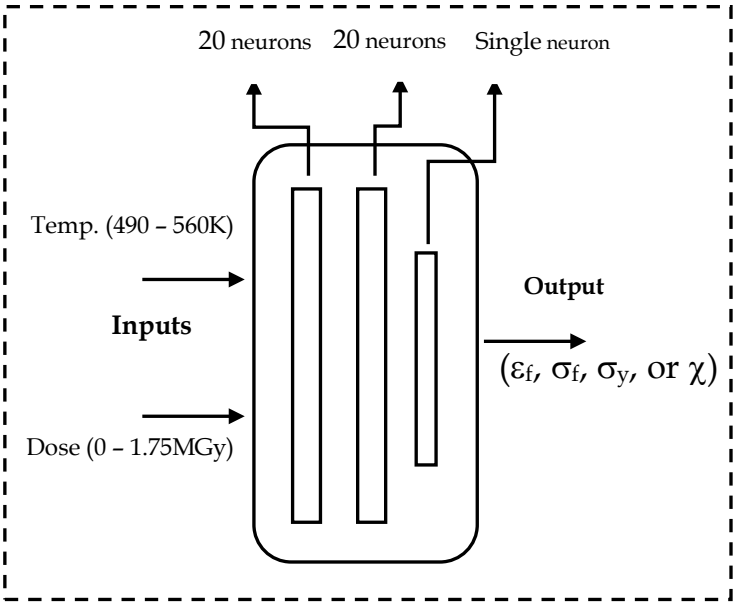

Fig. 5- A block diagram of the hardening characteristics- ANN based modeling.

The four proposed ANNs in this paper were trained using Levenberg-Marquardt optimization technique.
A two hidden layers network structure of 20 and 20 neurons respectively and the out put layer consisting of one neuron as in table 1. The selection of the optimal value of NN results was preformed by systemically changing its value in the training step (10 – fold cross-validation). In this training, 75% of the vectors are used to train the network and 25% of the vectors are used to validate how well the network generalized. Training was terminated after average sum square error of 1.4×10-2 was reached (50 epochs) for the four ANNs respectively. Different configurations of the four networks were investigated.

Number of training vectors	2948
Number of validation vectors	631
Number of testing vectors	631
Neurons of 1st hidden layer	20
Neurons of 2nd hidden layer	20
Training algorithm	Levenberg-Marquardt
Training epochs	50
Activation function of the hidden layers	Hyperbolic tangent
Activation function of the output layers	Linear

Table 1- Main information about the training of ANN model.

Simulation results based on ANN approach to modeling ε_f, σ_f, σ_y, and χ are given in Fig. 3. It can be seen from these figures that the trained (simulated) and predicted NN model shows almost exact fitting. Then, ANN model and Levenberg-Marquardt algorithm were used to calculate the nonlinear relationship between the temperature via, ε_f, σ_f, σ_y, and χ at different doses with almost exact accuracy. These results give the ANN provision of wide usage in modeling of mechanical properties of metals and alloys.

Acknowledgement

The authors would like to acknowledge financial support for this work from the Deanship of Scientific Research (DSR), University of Tabuk, Tabuk, Saudi Arabia, under grant no. S-0031-1434.

References

[1] S. Abis, G. Onofrio, Proceeding of Advanced Materials, Milano, Italy, (1989) 511.
[2] A.M. Abd El-Khalek; Materials Science and Engineering A 500 (2009) 176–181.
[3] F. Abd El-Salam, R.H. Nada, A.M. Abd El-Khalek, S.M. Abdou, AMSE 74 (2) (2001) 31.
[4] F. Abd El-Salam, A.M. Abd El-Khalek, R.H. Nadaa, L.A. Wahab, H.Y. Zahran; Materials Science and Engineering A 527 (2010) 1223–1229.

[5] A.M. Abd El-Khalek; Physica B, 315 (2002) 7–12.
[6] F.Abd EI-Salam, M.R. Nagy; Proc. Math. Phys. Soc. Egypt, 47, (1979)179–185.
[7] M.H.N. Beshai, G.H. Deaf, A.M. Abd El-Khalek, G. Graiss, and M.A. Kenawy; Phys. Stat. Sol. (a) 161 (1997) 65–72.
[8] P. Van Mourik, Th.H. Dekeijeser, E.J. Mittemeijer; Scripta Metall., 21 (1987) 361–367.
[9] A.M. Abd El-Khalek and F. Abd El-Salam; *Radiation Effects & Defects in Solids* 163, 10, (2008) 835–842.
[10] G.H. Deaf, M.H.N. Beshai, A.M. Abd El-Khalek, G. Graiss, M.A. Kenawy, Cryst. Res. Technol. 32 (1997) 3.
[11] A. Gaber, N. Afify, M.S. Mostafa; J. Phys. D 23 (1990) 1119.
[12] R.V. Nandedkar, A.K. Tyagi; In Metallic Glasses; T.R. Anantharaman, Ed. Trans. Tech. Pub. (1984) 165–174.
[13] M.Y. El-Bakry, A. Moussa, A. Radi, E. El-dahshan, M. Tantawy, Int. J. Sci. Eng. Res. 3 (8) (2012) 15–21.
[14] M.Y. El-Bakry, A. Moussa, A. Radi, E. El-dahshan, D.M. Habashy, G.Abbas Ehab, Int. J. Sci. Eng. Res. 1 (2) (2012) 5–11.
[15] G.M. Behery, A.A. El-Harby, M.Y. El-Bakry, Int. J. Soft Comput. Bioinf. 3 (1) (2012) 1–10.
[16] M.Y. El-Bakry, K.A. El-Metwally, Chaos Solitons Fractals 16/2 (2003) 279–285.
[17] M.Y. El-Bakry, M. El-Helly, Mostafa Y. El-Bakry, Trans. Comput. Sci. III LNCS 5300 (2009) 171–183.
[18] S.Haykin, Neural Networks and learning machine, 3rd ed. Prentic Hall, Upper Saddle River (2008).
[19] I.A. Basheer, M.Hajmeer, Journal of Microbial Methods 43 (2000) 3-31.
[20] Michael Negnevitsky, Artificial Intelligence: A Guide to Intelligent System, Addison Wesley, England, (2005).
[21] A.A.Attia , M.M.El-Nahas , M.Y.El-Bakry & D.M.Habashy , Neuran Networks Modeling for Refractive Indices Of Semi Conductors , Optics Communications 287 (2013) 140-144.
[22] R.H. Nada, D.M. Habashy, F. Abd El-Salam, Mahmoud Y. El-Bakry, A.M. Abd El-Khalek , E. Abd El-Reheim; Materials Science & Engineering A 567 (2013) 80–83.
[23] A. M. Abd El-Khalek; Materials Science and Technology, 24, 11 (2008) 1333.
[24] F. Abd El-Salam, A.M. Abd El-Khalek, R.H. Nadaa, L.A. Wahab, H.Y. Zahran; Materials Science and Engineering A 527 (2009) 281–286.
[25] K. V. Ravi and E. Philofsky: Metallurgical Trans. 2 (1971) 711.